J|A|C|S COMMUNICATIONS

Published on Web 11/18/2010

Functional Hollow Carbon Nanospheres by Latex Templating

Robin J. White,* Klaus Tauer, Markus Antonietti, and Maria-Magdalena Titirici

Max-Planck-Institut für Kolloid- und Grenzflaechenforschung, MPI Campus Golm, Am Muehlenberg, 14476 Golm, 14424 Potsdam, Germany

Received August 26, 2010; E-mail: robin.white@mpikg.mpg.de

Abstract: A facile and sustainable synthesis of hollow carbonaceous nanospheres is presented, offering a scalable and multifunctional route to the generation of useful nanocontainers, which critically possess the stability not offered by polymeric equivalents and functionality not afforded by other nanocarbons. Carbonization temperature provides a subtle but elegant mechanism to control structure and thereby hydrophobicity, nanopartitioning, and permeation between the inner and outer space.

Future nanotechnology depends importantly on the ability to synthesize new nanomaterials possessing distinct structural and functional features.[1] In this context hollow nanospheres are unique materials and have attracted much research and industrial interest, due to their special shape, low density, and large void space fraction. Hollow nanospheres are "*processable voids*", possessing excellent flow performance and high surface area, where the high internal volume provides a unique storage space or artificial reaction "*cell*".[2] Applications of such hollow "*bodies or pores*" are diverse; they can be utilized as delivery/protection devices for a wide range of biologically/pharmaceutically important moieties (e.g., drugs,[3] contrast imaging agents,[4] and DNA[5]), are attractive candidates for the heterogenization and structure direction of catalysts (e.g., in fuel cells),[6,7] and find use as templates[8] and adsorbents/detoxification media.[9]

In the context of the aforementioned applications, immense research interest has recently focused on the production of new high value hollow carbon-based nanomaterials, arising due to anticipated enhanced mechanical and electronic application performance. Current 2D and 3D carbon nanomaterials possess highly curved condensed aromatic/graphitic wall structuring and include nanotubes,[10] fullerenes,[10b,11] onions,[12] and nanocones.[13] These materials are however typically prepared in low yield, using expensive high vacuum techniques such as laser vaporization,[14] resistive heating,[15] or arc discharge methods,[16] with the products often lacking size or structure homogeneity, and hence are difficult to isolate and purify.[17] Furthermore, catalysts are often employed to access these materials at lower graphitization temperatures.[18] Here, we will focus on derivatives of hollow (graphitic) carbon nanospheres (HCS), owing to their proposed good electric conductivity, outstanding thermal stability, low density, and oxidation resistance at moderate temperature. In addition, we will describe control of additional, application relevant properties (e.g., surface functionality/degree of aromatic condensation (*vis-à-vis* surface polarity)).

Our group has previously exploited the hydrothermal carbonization (HTC) of a carbohydrate-based biomass under mild aqueous conditions for the production of a variety of useful functional carbonaceous nanomaterials,[19] including hollow micrometer-sized inorganic spheres,[20] and also the first versions of hollow but still weakly controlled HCS.[21] Given the technological importance of HCS, we decided to investigate the use of inexpensive renewable carbohydrate precursors (e.g., D-glucose) in combination with polymer latex templates, in the production of HCS via HTC, thus providing a simple multifaceted economical synthetic route which offers material property control in terms of surface chemistry/polarity, nanosphere size and shell thickness (Scheme 1). Homodisperse latex nanoparticles have been exploited previously for the synthesis of a wide range of hollow (inorganic) sphere materials.[2b,22] Latex nanoparticles can be readily prepared at a selectable size with a narrow size distribution allowing in principle subtle control of the hollow carbon nanosphere size over a wide range of diameters (e.g., below 150 nm). In this investigation hydroxyl terminated polystyrene latex (PSL) nanoparticles were selected as a suitable hydrogen bonding surface for the initial adsorption of HTC decomposition products, while the presence of sodium dodecyl sulfate (SDS) inhibits particle precipitation and association during the process. This approach also negates hazardous reagent use during the template extraction while the synthetic step is performed under relatively benign HTC conditions.

Scheme 1. Synthetic Strategy for the Synthesis Carbohydrate-Derived Hollow Carbonaceous Nanospheres

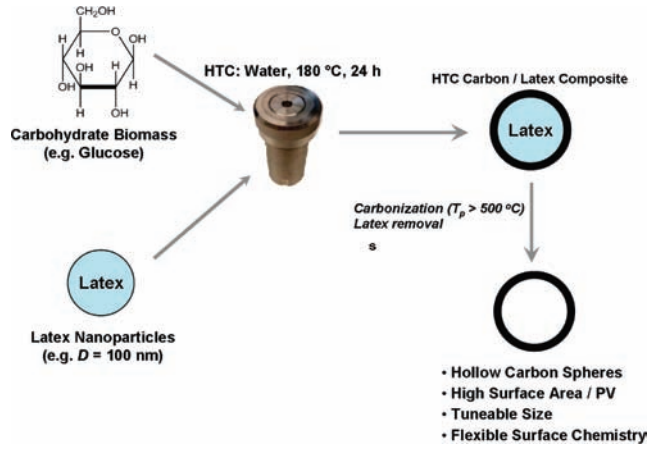

An aqueous dispersion of PSL of the desired size (e.g., D = 100 nm) is mixed with D-glucose acting as the carbon precursor (Scheme 1; Supporting Information). Our approach however is not limited to this model monomer, and in principle a broad variety of plant biomass-based products can be employed.[23] The system is then heated at 180 °C for 20 h. After reaction, the carbonaceous product can be filtered off, followed by washing with excess H_2O and drying under vacuum. To remove the polymer template and to graphitize the carbonaceous shell, the composite material is then heated to the desired temperature above the template decomposition point (e.g., >500 °C; Figure 1S Supporting Information) The

10.1021/ja107697s

Table 1. Textural and Chemical Properties of MPG-C Hollow Carbon Nanospheres[a]

Sample (T_p, °C)	[b]$S_{BET}{}^{N2}$, $m^2\ g^{-1}$	[c]$S_{area}{}^{Hg}$, $m^2\ g^{-1}$	[b]$V_{pore}{}^{N2}$, $cm^3\ g^{-1}$	[c]$V_{pore}{}^{Hg}$, $cm^3\ g^{-1}$	[c]Porosity, % ([d]ρ, g cm^{-3})	[e]% C, EA
MPG-C*100nm*	39	–	0.01	–	–	–
MPG-C*100nm*-550 °C	367	346	0.60	5.53	92.3(0.17)	85.9
MPG-C*100nm*-1000 °C	389	–	0.65	–	–	91.2
MPG-C*130nm*	52	–	0.01	–	–	–
MPG-C*130nm*-550 °C	466	435	1.60	3.84	86.5(0.23)	86.4

[a] S_{BET} = BET specific surface area. [b] N_2 sorption data. [c] Hg intrusion porosimetry data. [d] Density. [e] Elemental analysis data.

spherical hollow carbon nanosphere products are denoted as MPG-C*Xnm*-T_p, where X = template size (nm) and T_p = carbonization temperature (°C).

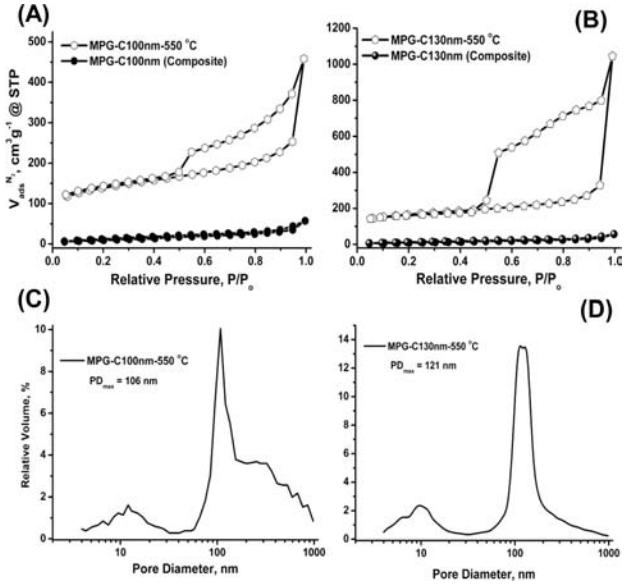

Figure 1. (A and B) N_2 sorption profiles for MPG-C hollow sphere materials before and after removal of polystyrene latex template; (C and D) H_g sorption pore size distributions for as-prepared hollow carbon sphere materials prepared at 550 °C (i.e., after template removal; PD_{max} indicates pore size maxima).

N_2 sorption profiles for representative template sizes investigated (i.e., 100 and 130 nm) demonstrate elegantly the development of material macroporosity as a result of template removal and the accessibility of the internal hollow carbon surface (Table 1; Figure 1A and B). The precursor composite materials recovered after initial HTC processing, MPG-C*100nm* and MPG-C*130nm*, show only a limited external surface. As a result of template thermolysis, a near 10-fold increase in the surface area was observed accompanied by a correspondingly large increase in pore volume, with specific surfaces areas (S_{BET}) calculated in excess of 350 $m^2\ g^{-1}$ for the two sizes investigated (e.g., $V_{pore}{}^{N2} > 0.6\ cm^3\ g^{-1}$; Table 1). Ink-bottle-type IV N_2 sorption profiles were observed, indicative of the complete filling of the hollow sphere morphology through the shell,[24] with the corresponding hysteresis loop area (expressing storage capacity) increasing as the template size enlarges from 100 to 130 nm (Figure 1A and B). Complementary Hg intrusion pore size distributions demonstrate the favorable replication of PSL nanoparticle template sizes used (Figure 1C and D). The maxima of the pore size distributions correspond well with the template size and distribution (e.g., MPG-C*100nm*-550 °C → 106 nm pore diameter maximum) (Figure 2S Supporting Information). The observed small shrinkage of the HCS diameter relative to template size is believed to be the result of shell contraction during carbon structure condensation at higher temperatures. The additional microporosity (apparent as the Y-axis intercept of the sorption isotherms) is indicative of small openings within the shell, which are also required to let template decomposition products leave the central cavity.

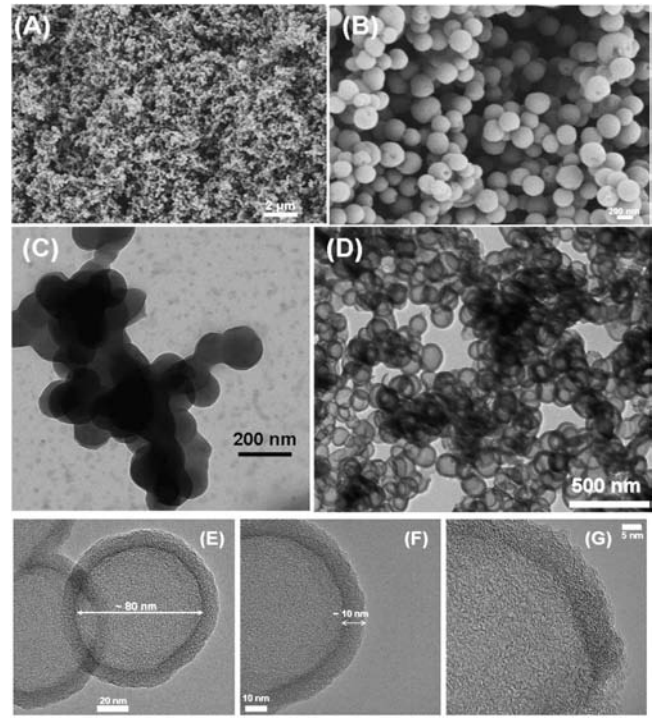

Figure 2. (A and B) SEM images of hydrothermal carbon/polystyrene latex nanoparticle composites for 100 and 130 nm templates respectively; (C) TEM images of MPG-C*100nm* HTC composite material (i.e., before template removal); (D) MPG-C*100nm*-550 °C demonstrating polystyrene latex template removal; (E, F, and G) HR-TEM images of MPG-C*100nm*-1000 °C.

SEM and TEM images depict the uniform coverage of PSL nanoparticles during HTC, demonstrating the MPG-C precursor composites present no internal void or hollow structure and a successful fusion of template and hydrothermal carbon, prior to template removal, although for the 130 nm templated sample some surface apertures are visible (Figure 2A−C). Carbonization at 550 °C results in complete template thermolysis yielding uniform replication and hollow carbonaceous spheres (e.g., MPG-C*100nm*-550 °C (Figure 2D). It could be anticipated that template decomposition in the sphere interior during thermolysis/carbonization may generate an associated pressure buildup within the sphere, and as a consequence some apertures or shell fragmentation would occur. Some shell rupture was observed but was by no means typical with the majority of the material (i.e., ~90%) presenting uniformly shaped hollow nanospheres, with a shell thickness of ~12 nm. This is presumably thin enough to allow for decomposition product escape through micropores without inducing significant shell damage.

As a further demonstration of the utility of our presented approach and also to investigate the thermal stability of the hollow spheres after template removal, the samples were also carbonized at 1000 °C (i.e., MPG-C*100nm*-1000 °C). The materials maintained practically identical N_2 sorption characteristics to MPG-C*100nm*-550 °C, with a slight increase in surface area/volume attributed to further carbon condensation to a more graphitic shell structure and a more thermally stable structure (Figure 2S Supporting Informa-

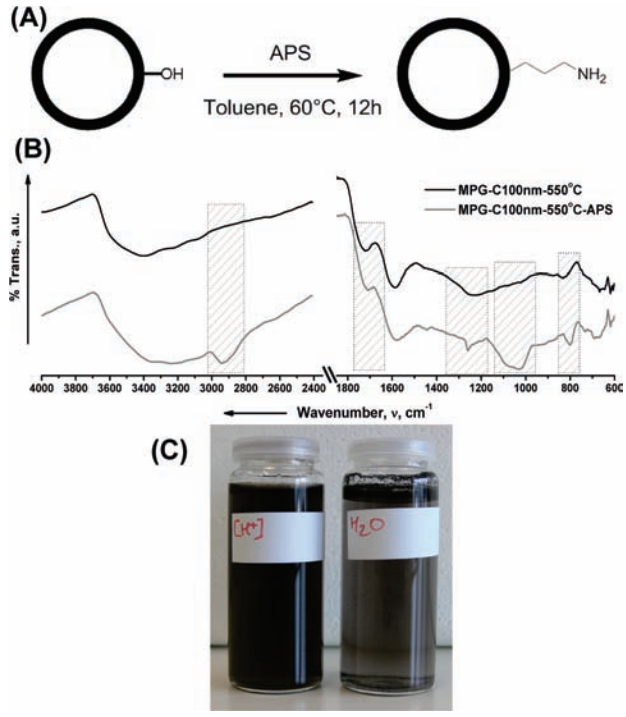

Figure 3. (A) Silylation scheme for modification of MPG-C*100nm*-550 °C with (3-aminopropyl) triethoxysilane (APS), (B) ATR FT-IR spectra of MPG-C*100nm*-550 °C and MPG-C*100nm*-550 °C + APS; and (C) Photograph of MPG-C*100nm*-550 °C + APS in (right) pure H_2O and (left) 1 M HCl (aq).

tion). HR-TEM imaging of MPG-C*100nm*-1000 °C indicates the maintenance of near perfect replication and 3D material stability after carbonization at this elevated temperature (Figure 2E−G). Internal particle diameters of ∼80 nm were measured, reflecting the further decrease in size relative to the template and the lower temperature material. The MPG-C*100nm*-1000 °C shell thickness was measured as ∼10 nm. Examination of the carbon shell by HR-TEM and XRD indicated a weakly ordered, bended form of graphitic carbon (Figure 2F and G and Figure 3S Supporting Information). It is anticipated that the graphitic ordering can be improved by altering the biomass source and/or coaddition of a graphitization catalyst, important for the proposed electrochemical applications.

Significantly the presented approach to HCS synthesis allows in principle the shell thickness to be easily adjusted by simply altering the relative ratio of sugar to latex template. Interestingly the generation of thinner shells by reducing sugar concentration or oppositely increasing template size would result in higher relative porosity and potentially lead to foam-like insulation materials. For modification of surface properties, miscibility or dispersibility, the standard functional groups of hydrothermal carbon can be favorably used to address a whole range of available functional groups.[25] This hydrothermal approach allows access to surfaces which are still rather hydrophilic and rich in C═O and C−OH functionalities. For illustration, a simple silylation of the oxygen containing functionality (e.g., −OH) at the MPG-C*100nm*-550 °C surface with (3-aminopropyl)triethoxysilane (APS; product termed MPG-C*100nm*-550 °C-APS) was used to introduce primary amine surface groups (Figure 3A).

Postmodification FT-IR analysis indicated the appearance of symmetric N−H and C−H stretching vibration bands in the 3000−2800 cm^{-1} region confirming the successful introduction of surface amino groups (Figure 3B), while elemental analysis confirmed the presence (4.1 wt % N) and loading density of the modifying group onto the hollow carbonaceous sphere (446 μg m^{-2}). Introduction of these amine groups allows the facile redispersion of the hollow spheres under acidic conditions to yield a stable aqueous dispersion (Figure 3C). It is emphasized that the presented approach is rather flexible in application. Introduction of secondary chemical additives to the HTC shell (e.g., a heteroatom source for N- or B-doping) would allow further chemical manipulation of the electronic properties of the hollow carbon nanospheres. Furthermore, the high porosities/low densities make these materials of particular interest for electrical and thermal/acoustic insulation applications, as a result of the potential ability to disperse and ultimately deploy these particles (e.g., pourable or sprayable "*pores*"). Size, chemical functionality, and in principle wall thickness can all be easily manipulated simply by variation of component concentration.

In summary, a facile, inexpensive, and sustainable synthesis of carbohydrate-derived hollow carbonaceous nanospheres was presented. This approach offers a relatively simple route to the production of useful nanocontainers, which critically possess the stability not offered by polymeric equivalents and functionality not afforded by other nanocarbons. This approach provides the basis for the generation of a simple yet multidimensional synthetic route to tunable functional hollow carbons, where carbonization temperature provides a subtle but elegant mechanism to control carbon structure and thereby hydrophobicity, nanopartitioning, and permeation between the inner and outer space.

Acknowledgment. The Max Planck Society is gratefully acknowledged for financial support. L. Zhao, J. Popovic, R. Pitschke, S. Pirok, and I. Shekova are thanked for the help with electron microscopy, XRD, elemental analysis, and TGA. Dr. N. Yoshizawa (AIST, Japan) is especially thanked for acquiring HR-TEM images. Dr. D. Enke (Universität Halle, Germany) is thanked for performing Hg intrusion porosimetry. R. Rothe is thankfully acknowledged for all her technical assistance. Dr. J. Roeser is extensively thanked for all his assistance. We acknowledge C. Briel and Erich C. for their contributions to discussions.

Supporting Information Available: Further experimental and characterization details, (i.e., thermogravimetric, particle size distribution, and X-ray diffraction analysis) for presented materials. This material is available free of charge via the Internet at http://pubs.acs.org.

References

(1) (a) Burda, C.; Chen, X. B.; Narayanan, R.; El-Sayed, M. A. *Chem. Rev* **2005**, *105* (4), 1025. (b) White, R. J.; Luque, R.; Budarin, V. L.; Clark, J. H.; Maquarrie, D. J. *Chem. Soc. Rev.* **2009**, *38*, 2–481.

(2) (a) Meier, W. *Chem. Soc. Rev* **2000**, *29* (5), 295. (b) Caruso, F. *Chem.—Eur. J.* **2000**, *6*, 3–413.

(3) (a) Gill, I.; Ballesteros, A. *J. Am. Chem. Soc.* **1998**, *128* (34), 8587. (b) Chen, J. F.; Ding, H. M.; Wang, J. X.; Shao, L. *Biomaterials* **2004**, *25*, 723. (c) Zhu, Y.; Shi, J.; Shen, W.; Dong, X.; Feng, J.; Ruan, M.; Li, Y. *Angew. Chem., Int. Ed.* **2005**, *44*, 5083. (d) Cai, Y.; Pan, H.; Xu, X.; Hu, Q.; Li, L.; Tang, R. *Chem. Mater.* **2007**, *19*, 3081.

(4) (a) Buchold, D. H. M.; Feldmann, C. *Nano Lett.* **2007**, *7*, 3489. (b) Chen, J.; Saeki, F.; Wiley, B. J.; Cang, H.; Cobb, M. J.; Li, Z. Y.; Au, L.; Zhang, H.; Kimmey, M. B.; Li, X. D.; Xia, Y. *Nano Lett.* **2005**, *5*, 473.

(5) Zelikin, A. N.; Li, Q.; Caruso, F. *Angew. Chem., Int. Ed* **2006**, *45*, 7743.

(6) (a) Mathiowitz, E.; Jacob, J. S.; Jong, Y. S.; Carino, G. P.; Chickering, D. E.; Chaturvedi, P.; Santos, C. A.; Vijayaraghavan, K.; Montgomery, S.; Bassett, M.; Morrell, C. *Nature* **1997**, *386*, 410. (b) Liang, H. P.; Zhang, H. M.; Hu, J. S.; Guo, Y. G.; Wan, L. J.; Bai, C. L. *Angew. Chem., Int. Ed.* **2004**, *43*, 1540. (c) Cheng, L. Q.; Liu, Y. L.; Zhang, J. X.; Yuan, D. S.; Xu, C. W.; Sun, G. H. *Prog. Chem.* **2006**, *18*, 1298.

(7) Chen, H. M.; Liu, R. S.; Lo, M. Y.; Chang, S. C.; Tsai, L. D.; Peng, Y. M.; Lee, J. F. *J. Phys. Chem. C* **2008**, *112* (20), 7522.

(8) Caruso, F.; Caruso, R. A.; Möhwald, H. *Science* **1998**, *282*, 1111.

(9) Joncheray, T. J.; Audebert, P.; Schwartz, E.; Jovanovic, A. V.; Ishaq, O.; Chávez, J. L.; Pansu, R.; Duran, R. S. *Langmuir* **2006**, *22*, 8684.

(10) (a) Saito, Y.; Hamaguchi, K.; Hata, K.; Uchida, K.; Tasaka, Y.; Ikazaki, F.; Yumura, M.; Kasuya, A.; Nishina, Y. *Nature* **1997**, *389*, 554. (b) Dai, L.; Mau, A. W. H. *Adv. Mater.* **2001**, *13*, 12–899. (c) Zhao, W.; Song, C.; Pehrsson, P. E. *J. Am. Chem. Soc.* **2002**, *124* (42), 12418.
(11) Kroto, H. W.; Heath, J. R.; O'Brien, S. C.; Curl, R. F.; Smalley, R. E. *Nature* **1985**, *318*, 162.
(12) (a) Banhart, F.; Ajayan, P. M. *Nature* **1996**, *382*, 433. (b) Banhart, F.; Fuller, T.; Redlich, P.; Ajayan, P. M. *Chem. Phys. Lett.* **1997**, *269*, 349. (c) Chen, X. H.; Deng, F. M.; Wang, J. X.; Yang, H. S.; Wu, G. T.; Zhang, X. B.; Peng, J. C.; Li, W. Z. *Chem. Phys. Lett.* **2001**, *336*, 201.
(13) (a) Krishnan, A.; Dujardin, E.; Treacy, M. M. J.; Hugdahl, J.; Lynum, S.; Ebbesen, T. W. *Nature* **1997**, *388*, 451. (b) Sattler, K. *Carbon* **1995**, *33*, 7–915.
(14) (a) Guo, T.; Nikolaev, P.; Thess, A.; Colbert, D. T.; Smalley, R. E. *Chem. Phys. Lett.* **1995**, *243* (1), 49. (b) Schauerman, C. M.; Alvarenga, J.; Landi, B. J.; Cress, C. D.; Raffaelle, R. P. *Carbon* **2009**, *47*, 10–2431.
(15) (a) Ugarte, D. *Nature* **1992**, *359*, 707. (b) Kizuka, T.; Kato, R.; Miyazawa, K. *Carbon* **2009**, *47*, 1–138.
(16) (a) Iijima, S. *Nature* **1991**, *354*, 56. (b) Sano, N.; Wang, H.; Alexandrou, I.; Chhowalla, M.; Teo, K. B. K.; Amaratunga, G. A. J.; Iimura, K. *J. Appl. Phys.* **2002**, *92*, 5–2783.
(17) Georgakilas, V.; Voulgaris, D.; Vázquez, E.; Prato, M.; Guldi, D. M.; Kukovecz, A.; Kuzmany, H. *J. Am. Chem. Soc.* **2002**, *124* (48), 14318.
(18) (a) Herring, A. M.; McKinnon, J. T.; McCloskey, B. D.; Filley, J.; Gneshin, K. W.; Pavelka, R. A.; Kleebe, H. J.; Aldrich, D. J. *J. Am. Chem. Soc.* **2003**, *125*, 9916. (b) Li, G.; Guo, C.; Sun, C.; Ju, Z.; Yang, L.; Xu, L.; Qian, Y. *J. Phys. Chem. C* **2008**, *112*, 1896.
(19) (a) Yu, S. H.; Cui, X. J.; Li, L. L.; Li, K.; Yu, B.; Antonietti, M.; Colfen, H. *Adv. Mater.* **2004**, *16* (18), 1636. (b) Titirici, M. M.; Thomas, A.; Antonietti, M. *New J. Chem.* **2007**, *31*, 6–787. (c) Makowski, P.; Demir-Cakan, R. D.; Antonietti, M.; Goettmann, F.; Titirici, M. M. *Chem. Commun.* **2008**, 999. (d) Demir-Cakan, R. D.; Hu, Y. S.; Antonietti, M.; Maier, J.; Titirici, M. M. *Chem. Mater.* **2008**, *20*, 4–1227. (e) Hu, Y. S.; Demir-Cakan, R. D.; Titirici, M. M.; Antonietti, M.; Mueller, J. O.; Schloegl, R.; Maier, J. *Angew. Chem., Int. Ed.* **2008**, *47*, 9–1645.
(20) Titirici, M. M.; Antonietti, M.; Thomas, A. *Chem. Mater.* **2006**, *18* (16), 3808.
(21) Cui, X. J.; Antonietti, M.; Yu, S. H. *Small* **2006**, *2* (6), 756.
(22) (a) Antonietti, M.; Berton, B.; Goltner, C.; Hentze, H. P. *Adv. Mater.* **1998**, *10* (2), 154. (b) Caruso, F.; Caruso, R. A.; Mohwald, H. *Chem. Mater.* **1999**, *11*, 3309. (c) Xia, Y.; Gates, B.; Yin, Y.; Lu, Y. *Adv. Mater.* **2000**, *12*, 10–693. (d) Tissot, I.; Reymond, J. P.; Lefebvre, F.; Bourgeat-Lami, E. *Chem. Mater.* **2002**, *14*, 3–1325. (e) Agrawal, M.; Gupta, S.; Pich, A.; Zafeiropoulos, N. E.; Stamm, M. *Chem. Mater.* **2009**, *21*, 5343.
(23) (a) Titirici, M. M.; Antonietti, M.; Baccile, N. *Green Chem* **2008**, *10* (11), 1204. (b) Titirici, M. M.; Antonietti, M. *Chem. Soc. Rev.* **2010**, *39*, 1–103. (c) Hu, B.; Wang, K.; Wu, L.; Yu, S. H.; Antonietti, M.; Titirici, M. M. *Adv. Mater.* **2010**, *22*, 7–813.
(24) Ravikovitch, P. I.; Neimark, A. V. *Langmuir* **2002**, *18*, 9830.
(25) Titirici, M. M.; Thomas, A.; Antonietti, M. *J. Mater. Chem* **2007**, *17* (32), 3412.

JA107697S